Kondo physics in a Ni impurity embedded in O-doped Au chains

S. Di Napoli,[1,2] M. A. Barral,[1,2] P. Roura-Bas,[1,2] L. O. Manuel,[2,3] A. M. Llois,[1,2] and A. A. Aligia[4]

[1]*Departamento de Física de la Materia Condensada, GIyA-CNEA, Avenida General Paz 1499, (1650) San Martín, Provincia de Buenos Aires, Argentina*

[2]*Consejo Nacional de Investigaciones Científicas y Técnicas, CONICET, 1033 Buenos Aires, Argentina*

[3]*Instituto de Física Rosario (CONICET-UNR), 2000 Rosario, Argentina*

[4]*Centro Atómico Bariloche and Instituto Balseiro, Comisión Nacional de Energía Atómica, 8400 Bariloche, Argentina*

(Received 12 May 2015; revised manuscript received 29 July 2015; published 12 August 2015)

By means of *ab initio* calculations we study the effect of O doping of Au chains containing a nanocontact represented by a Ni atom as a magnetic impurity. In contrast to pure Au chains, we find that with a minimum O doping the $5d_{xz,yz}$ states of Au are pushed up, crossing the Fermi level. We also find that for certain O configurations, the Ni atom has two holes in the degenerate $3d_{xz,yz}$ orbitals, forming a spin $S = 1$ due to a large Hund interaction. The coupling between the $5d_{xz,yz}$ Au bands and the $3d_{xz,yz}$ of Ni states leads to a possible realization of a two-channel $S = 1$ Kondo effect. While this kind of Kondo effect is commonly found in bulk systems, it is rarely observed in low dimensions. The estimated Kondo scale of the system lies within the present achievable experimental resolution in transport measurements. Another possible scenario for certain atomic configurations is that one of the holes resides in a $3d_{z^2}$ orbital, leading to a two-stage Kondo effect, the second one with SU(4) symmetry.

DOI: 10.1103/PhysRevB.92.085120 PACS number(s): 73.23.Hk, 71.10.Hf, 75.20.Hr

I. INTRODUCTION

In modern nanoscience, tailoring the electronic transport through atomic-size conductors has turned into a duty, as it is a powerful tool for detecting nanomagnetism. Atomic-size contacts can be experimentally obtained by different techniques, particularly in a mechanically controllable break junction (MCBJ) experiment, where the formation of one-dimensional atomic chains of several kinds of elements is possible [1–6]. Since the achievement of the first freestanding atomic chains of gold atoms in 1998 [2,3], the search for other elements that could also form atomic chains has been intense and active. For instance, in the last few years it has been possible to strengthen the bonds in a suspended chain and to achieve a higher probability of chain producibility by adding external absorbates during the chain formation process. It is known that low-coordinated atoms are chemically more reactive than in bulk [7]; thus, chains are expected to be even more reactive than nanoparticles, opening the possibility for molecular absorbates to dissociate, even at low temperatures. For instance, oxygen (O) atoms are expected to be incorporated in the chains, as predicted in several previous works [8–13].

Due to outstanding experimental achievements in the last decades, it is nowadays possible to design nanodevices as tools for detecting nanomagnetism by conductance measurements through atomic metal contacts. One can indirectly sense the presence of magnetism by detecting zero-bias anomalies, usually originated in the Kondo screening of the spin, if a magnetic impurity is bridging the contact.

In previous works, Lucignano *et al.* [14] and Miura *et al.* [15] studied the electronic structure and the Kondo conductance through a Ni impurity embedded in a monoatomic Au wire. The Ni atom in the Au chain has two low-energy geometries: bridge (B) and substitutional (SUB). While in the B configuration, the usual one-channel Kondo (1CK) effect of spin $S = 1/2$ was reported theoretically, no Kondo physics was predicted in the SUB configuration. This is due to the fact that in the SUB geometry (of higher total energy but probably accessible at large stress, as is the case in a MCBJ experiment), the empty spin-down Ni state orbitals are a $3d_{xz,yz}$ degenerate pair with angular momentum projection $|m| = 1$. In this geometry the Ni impurity has $S \simeq 1$ and these magnetic orbitals are "spectators" as they cannot be screened due to their orthogonality to the $m = 0$ Au conduction band. Indeed, transport experiments in Au chains indicate that the conduction channel is a single $6s$ band [16,17]. We remind the reader that the Kondo effect requires that band states of the same symmetry of the localized states lie at the Fermi energy.

As was previously mentioned, O impurities in the Au chain are expected during its real formation under an open atmosphere. A dramatic effect of the incorporated O impurities to the Au chains was found in our recent *ab initio* calculations [18]. They can modify the band structure of the metallic host, pushing up the bands that are close to the Fermi level, thus establishing conduction through the $5d_{xz}$ and $5d_{yz}$ electrons of Au. In these conditions, the spin of the Ni impurity, in the SUB geometry, formed by the localized $3d_{xz,yz}$ electrons, can be screened by conduction electrons of the O-doped Au chain and Kondo physics is expected. A similar feature was obtained in O-doped Au chains containing a magnetic $S = 3/2$ Co impurity [19,20]. Remarkably, the examples of Ni-Au-O and Co-Au-O systems are expected to be realizations of Kondo models where an arbitrary spin S is screened by n channels, and were solved exactly by the Bethe ansatz [21–24]. For $n = 2S$ the models present Fermi liquid properties, while for $n > 2S$ non-Fermi-liquid behavior is obtained and for $n < 2S$ the systems are singular Fermi liquids [25]. We must warn the reader that the non-Fermi-liquid behavior requires SU(n) symmetry which is difficult to achieve in real systems. For the $S = 1/2$ two-channel model, the effect of several symmetry-breaking perturbations was discussed by Sela *et al.* [26]. The presence of anisotropy also modifies the low-temperature behavior [19,20,27,28].

In this paper, we focus on a Ni magnetic impurity embedded, in a SUB configuration, within an O-doped Au chain. We study the effects of the presence of O impurities on the symmetry of the Au conduction bands close to the Fermi level as well as on the spin state of the Ni impurity. This symmetry determines the nature of the screening of the impurity spin, giving rise to the possibility of the system to exhibit some kind of Kondo effect. In particular, we found a stable configuration in which the model that describes the system corresponds to a spin $S = 1$ screened by two conduction channels. Using parameters coming from *ab initio* calculations, we build the model Hamiltonian which corresponds to a generalized Anderson impurity model. After a Schrieffer-Wolff transformation we prove that the effective low energy model is a $S = 1$, 2-channel Kondo model. We analyze this model at zero temperature and give an estimation of the expected Kondo temperature (T_K) for this system.

For other atomic configurations, corresponding to metastable states, the *ab initio* results suggest a sixfold degenerate ground state of the Ni atom, with one hole in a $3d_{z^2}$ orbital and another one in either a $3d_{xz}$ or a $3d_{yz}$ orbital in an $S = 1$ state. This is analogous to the situation of Fe iron(II) phtalocyanine molecules on Au(111), where a two-stage Kondo effect takes place, screening first the spin 1/2 of the $3d_{z^2}$ hole and then that of the orbitally degenerate remaining hole in an SU(4) Kondo effect [29].

The paper is organized as follows. In Sec. II we provide the details of our DFT first-principles calculations and show the band structure for the different hosts and the consequences of these structures on the systems with an embedded Ni impurity. Some effect of correlations in the Ni $3d$ shell are discussed in Sec. III. In Sec. IV we present the Kondo model, obtained by a Schrieffer-Wolff transformation of the $S = 1$ two-channel Anderson model, and obtain the Kondo temperature. Finally, a summary and discussion are given in Sec. V.

II. *Ab initio* RESULTS: SYMMETRY OF THE Au CONDUCTION BANDS AND Ni HOLES

We perform *ab initio* calculations based on density functional theory (DFT) using the full potential linearized augmented plane waves method, as implemented in the WIEN2K code [30]. The generalized gradient approximation for the exchange and correlation potential in the parametrization of PBE [31] and the augmented plane waves local orbital basis are used. The cutoff parameter which gives the number of plane waves in the interstitial region is taken as $R_{mt} K_{\max} = 7$, where $K_{\max}$ is the value of the largest reciprocal lattice vector used in the plane waves expansion and R_{mt} is the smallest muffin-tin radius used. The number of **k** points in the Brillouin zone is enough, in each case, to obtain the desired energy and charge precisions, namely 10^{-4} Ry and 10^{-4} e, respectively. The muffin-tin radii were set to 2.23 bohrs for Ni, 1.91 bohrs for Au atoms, and 1.69 bohrs for the O impurities.

In all the studied cases we consider a simple hexagonal lattice with the chains aligned in the z direction. The lattice parameter c depends on the number of atoms of the considered chains and the lattice parameter in the x,y plane a $(=b)$ = 15 bohrs was checked to be large enough to avoid artificial interactions between the periodic replicas of the wire. We have chosen a hexagonal cell (and not a tetragonal one, for example) because the splitting of the Ni $3d$ orbitals is the same as that of the isolated wire. In other words, the $3d$ orbitals split into the same irreducible representations in the point groups D_{6h} and $D_{\infty h}$ (or C_{6v} and $C_{\infty v}$ if the horizontal x,y plane of symmetry is lacking).

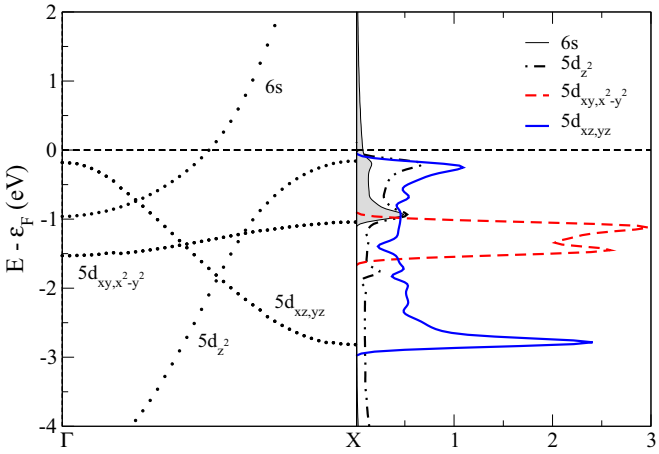

FIG. 1. (Color online) Electronic band structure (left) and orbitally decomposed projected density of states (PDOS) per spin (right) of the Au monoatomic chain at the GGA equilibrium distance $d^{eq}_{\text{Au-Au}} = 4.9285$ bohr. The Hubbard U parameter set in this calculation is $U = 4$ eV.

As a first step, we analyze the case of a Au monoatomic chain and its band structure. Usually, DFT calculations yield a spurious magnetization in Au wires, due to self-interaction errors, which shift the $5d_{xz,yz}$ ($|m| = 1$) bands of the Au wire up to the Fermi energy. One route to avoid this spurious result is to increase the Au-Au distance in the chains during the calculations [14,15]. We pick up another route to tackle this problem and, as suggested by Sclauzero and Dal Corso [32], we include a Hubbard U correction of $U = 4$ eV in the $5d$-electron Au manifold. It is noteworthy to say that with the additional energy gap the Au chain restores the experimental conductance properties. In the calculations reported in Fig. 1, the above mentioned magnetization is completely suppressed in the chain at the equilibrium distance of $d^{eq}_{\text{Au-Au}} = 4.9285$ bohrs.

In O-doped Au chains, we relax the Au-O distance for the case of AuO diatomic chain (two-atom unit cell) and, afterwards, we take the same bond length, $d^{eq}_{\text{Au-O}} = 3.625$ bohrs, for all the studied chains. We consider several O dopings to find which the minimal amount of O is needed to push the projected $5d_{xz,yz}$ density of states of all Au atoms towards the Fermi level. In this way, the $|m| = 1$ symmetry conduction channel through all the Au atoms in the chain is opened. In all the studied cases—i.e., 50% (AuO), 33.3% (Au_2O), 25% (Au_4O), and 14% (Au_6O)—we include the same Hubbard $U = 4$ eV in the $5d$ electrons of Au and perform self-consistent calculations. We find that the $5d_{xz,yz}$ orbitals of Au, up to the third neighbors of the O impurity, cross the Fermi level, due to the large hybridization with the oxygen $2p_{x,y}$ states. This is shown in Fig. 2, where we plot the $5d_{xz,yz}$ density of states of the Au atom located farthest away from the O atoms, for some selected dopings. From this we can conclude that an O doping

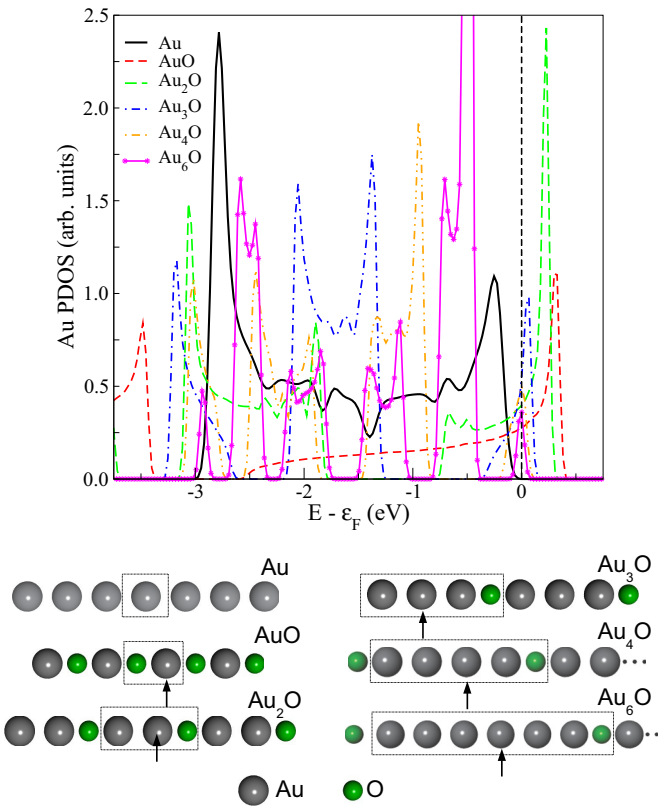

FIG. 2. (Color online) Top: $5d_{xz,yz}$ projected density of states of the Au atom located farthest away from the O atom. Bottom: Schematic representation of the chains. The unit cell is shown for each case and the arrows indicate the Au atom whose projected density of states is shown in the top panel.

of 14% is enough to transform the Au bands into conducting channels. We consider below a doping of ≈19% (3/16).

Once the minimum amount of O present in the Au chains is set, we include the Ni impurity in our calculations. The question that arises then is where to put the O atoms and the Ni impurity within the Au chain. We assume that the O atoms are not bonded to the Ni impurity and relax the Au-Ni bond length for a diatomic Ni-Au chain, giving $d^{eq}_{\text{Au-Ni}} = 4.4805$ bohrs, in excellent agreement, within 0.05%, with that obtained by Miura *et al.* [15]. For a chain containing 12 Au atoms, 3 O atoms, and 1 Ni impurity within the unit cell, we take the corresponding bond lengths as $d^{eq}_{\text{Au-Ni}} = 4.4805$ bohrs, $d^{eq}_{\text{Au-O}} = 3.625$ bohrs, and $d^{eq}_{\text{Au-Au}} = 4.9285$ bohrs. In consequence, the Ni-Ni distance in the z direction is larger than 70 bohrs and, therefore, we assume that the Ni-Ni magnetic interaction is negligible.

To find out if the O's position, with respect to the Ni atom, changes the spin-state of the Ni impurity or its hole's symmetries, we explore several configurations, always keeping the same amount of O in the Au chain. In Table I we introduce the different cases studied and their corresponding Ni magnetic moments as well as the occupation numbers (in electrons) obtained by integrating the minority band separated in the different symmetries, within the Ni-muffin-tin sphere. The last entry corresponds to a metastable solution, whose energy is 85 meV higher than that of the previous entry. Note that for the $3d_{z^2}$ symmetry the maximal occupation could be as much as $n(3d_{z^2}) = 1$, whereas $n(3d_{xy,x^2-y^2}) = n(3d_{xz,yz}) \leqslant 2$ as they both are twofold-degenerate states. Based on the data shown in the table, we can distinguish between two extreme cases for the stable solutions: the one called "sym O–4th nn" and the one denominated "sym O–2nd nn". In the former case, the Ni atom is placed in the center of the O-doped Au chain and it has two O atoms symmetrically located as fourth neighbors. The $3d_{z^2}$ orbital is almost completely filled and the twofold-degenerate orbitals $3d_{xz,yz}$ are almost empty. As the O atoms approach the Ni impurity, the $3d_{xz,yz}$ orbitals increase their filling while the $3d_{z^2}$ orbital moves towards the Fermi level decreasing its occupancy until it becomes almost half filled in the case called "sym O–2nd nn". In this last case, the Ni impurity has two O atoms at second-neighbor positions. Note that for the metastable configuration, with one O atom as third and another as fourth nearest neighbors ("no-sym 1O–3rd nn"), the minority $3d_{z^2}$ state is almost empty. The small energy difference (85 meV) between the metastable and stable configurations suggests a near degeneracy between the triplet of the Ni $3d^8$ configuration with two holes occupying the $m = \pm 1$ states (or $3d_{xz,yz}$ orbitals) and the two triplets with one hole in the $m = 0$ ($3d_{z^2}$) state and another one with $m = \pm 1$. In the calculations there is always a finite splitting, larger than 0.5 eV, positive or negative of the peaks in the minority spectral density for $m = 0$ and $m = \pm 1$, but this is probably due to the exchange and correlation potential included in the DFT, since a partial occupation of one state pushes the other up in energy.

In Fig. 3 we show the partial density of states projected onto the different symmetries of the Ni impurity, for two of the above mentioned cases. The Ni impurity develops a magnetic moment of $\mu_{\text{Ni}} = 1.37\mu_B$ in the "sym O–4th nn" configuration and, as also found for the Ni impurity embedded in a Au monowire [15], the Au atoms at both sides of the Ni atom develop a small induced magnetic moment of around $0.18\mu_B$. The calculated Ni magnetic moment is $\mu_{\text{Ni}} = 1.33\mu_B$ in the "sym O–2nd nn" case, and the induced magnetic moment in the Au atoms located at both sides of the Ni impurity is around $0.31\mu_B$. The enhancement of this last induced magnetic moment is due to the proximity of the O atoms [See sketch of Fig. 3(b)].

In spite of the fact that the spin state of the Ni impurity in both configurations is almost the same, the hole's symmetries are different. It can be seen from Fig. 3(a) that the empty spin-down Ni orbitals (holes) are the $3d_{xz,yz}$, while the other orbitals remain occupied. The different band fillings change, depending on the position of the O impurities. Upon approaching the O atoms towards the Ni impurity, the $3d_{xz,yz}$ orbitals begin to be filled, while the $3d_{z^2}$ one begins to be unoccupied, as shown in Fig. 3(b). One also observes in this figure that the minority $3d_{z^2}$ state lies at the Fermi level and the density corresponding to the $3d_{xz,yz}$ states is split in two around the Fermi level, suggesting a near degeneracy of the $m = 0$ and $m = \pm 1$ states as in the case when the O atoms are third and fourth nearest neighbors of Ni, already discussed above. In all the treated cases, the $3d_{xy,x^2-y^2}$ states are the most localized, as they lie perpendicular to the chain, thus having a small hybridization. Nevertheless, we observe that the position of these filled degenerate orbitals might change depending on O proximity.

TABLE I. Symmetry-dependent d-band minority spin fillings of the Ni atoms (in electrons) for the selected studied cases. The color coding of the schematic representation of the chains is the one presented in Fig. 3(a).

Case	Unit cell's schema	$n(3d_{z^2})$	$n(3d_{xy,x^2-y^2})$	$n(3d_{xz,yz})$	$\mu_{\rm Ni}(\mu_B)$
sym O-4th nn		0.92	1.87	0.56	1.37
sym O-3rd nn		0.86	1.69	1.00	1.11
sym O-2nd nn		0.63	1.60	1.21	1.33
no-sym 1O-2nd nn		0.67	1.58	1.18	1.31
no-sym 1O-3rd nn		0.91	1.82	0.72	1.26
idem above metastable		0.27	1.53	1.67	1.26

In order to determine the anisotropy constant D, taken into account in the term $H_D = DM_2^2$ of the Hamiltonian defined in Eq. (1) of Sec. IV, we introduce the spin-orbit interaction in the Ni impurity and perform self consistent calculations within the fully relativistic approximation. For the "sym O–4th nn" case we obtain a magnetocrystalline anisotropy energy, MAE, equal to $E_\parallel - E_\perp \sim 10$ meV, where $E_\parallel$ ($E_\perp$) is the total energy corresponding to the total magnetization pointing along (perpendicular to) the chain's axis. Therefore, we obtain that the easy magnetization axis is perpendicular to the chain. To calculate the value of D we proceed as in Ref. [33]. The expectation value of the anisotropy in the state $|11\rangle$ of maximum projection in the z direction is clearly $\langle 11|H_D|11\rangle = D$. By rotating this state, one obtains that the state of maximum projection in the x direction is $|11x\rangle = |10\rangle/\sqrt{2} + (|11\rangle + |1-1\rangle)/2$, and $\langle 11x|H_D|11x\rangle = D/2$. From the energy difference $D \sim 20$ meV.

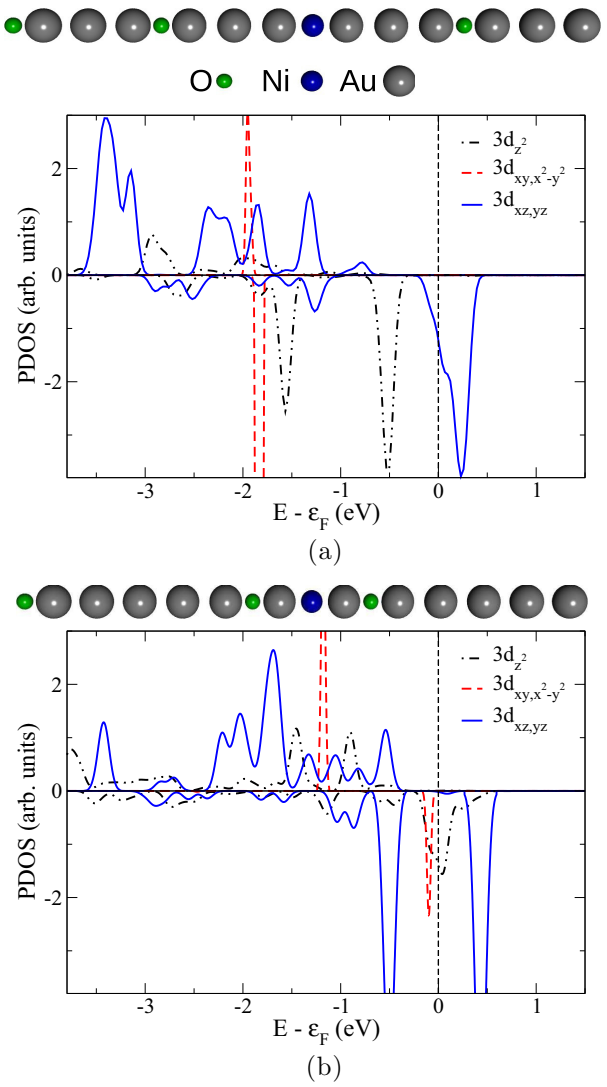

FIG. 3. (Color online) Ni impurity in a 19% O-doped Au chain. In each case, the unit cell and the density of states projected onto different symmetries are shown. (a) Case "sym O–4th nn": Two O atoms are symmetrically positioned as Ni-fourth neighbors. (b) Case "sym O–2nd nn": Two O atoms as Ni-second neighbors.

III. EFFECTS OF CORRELATIONS IN Ni

In this section we investigate the effects of correlations in an isolated $3d^8$ configuration on the relative stability of the two possible ground states discussed above: spin triplet with total angular momentum projection $L_z = 0$ with one hole with $m = 1$ and the other with $m = -1$, or two triplets with $L_z = \pm 1$ (one hole with $m = 0$ and the other with $m = \pm 1$). We also provide an alternative estimation of the anisotropy parameter D. Since the GGA underestimates correlations that affect the orbital polarization of the d states [34–37], this calculation is an important complement to the *ab initio* results presented above.

The $3d^8$ configuration has 45 different states (the number of ways to put two indistinguishable holes in 10 spin-orbitals). The second quantized form of the Coulomb repulsion written in the basis of the 10 spin-orbitals contains many different terms (density-density, exchange, and hopping of pairs involving different orbitals) but can be parametrized in terms of three Coulomb integrals F_0, F_2, and F_4 [37,38]. We have solved exactly the 45×45 matrix of the Hamiltonian corresponding to the $3d^8$ configuration, containing crystal-field splitting and all the above mentioned Coulomb terms in the d shell, as described for example in Refs. [37,38]. In a later step, to calculate D, we include the spin-orbit coupling $\hat{H}_{\rm SOC} = \lambda \sum_i \hat{\mathbf{l}}_i \cdot \hat{\mathbf{s}}_i$. We have considered the Coulomb integrals $F_2 = 0.16$ eV, $F_4 = 0.011$ eV, and $\lambda = 0.08$ eV from a fit of the low-energy spectra of late transition metal atoms. F_0 does not modify the differences between energies within one configuration.

For the crystal-field splitting, we took two different sets of parameters. From the *ab initio* results presented in

Fig. 3(a) for the minority states, we estimate -1.85, -1, and -0.3 eV for the on-site energy of the states with $m = \pm 2$, 0, and ± 1, respectively. For the latter, which is unoccupied, we have subtracted a correlation term included in the GGA, which we estimate to be 0.5 eV. In the second set we assume that the $m = 0$ and $m = \pm 1$ states are degenerate, with the same average distance to the $m = \pm 2$ states as before. This is equivalent to take -1.2 eV for the energy of the electrons with $x^2 - y^2$ and xy symmetry and 0 for the remaining three. Note that in the last case, in the absence of interactions, the above mentioned two-hole possible ground states with $L_z = 0$ and $L_z = \pm 1$ are degenerate. We find that interactions stabilize the triplet with $L_z = 0$ by 0.30 eV. For the first set of parameters, the stabilization energy for this triplet, which is 0.7 eV in the absence of interactions, is increased to 0.88 eV in the present calculation. The difference 0.18 eV can be ascribed to the effect of correlations.

When spin-orbit is included we obtain $D = 8.5\,(16.7)$ meV for the first (second) set of parameters. The sign and order of magnitude agree with the *ab initio* results.

IV. Ni IMPURITY WITHIN AN O-DOPED Au CHAIN: KONDO EFFECT

According to the results of the previous section, different model Hamiltonians can be formulated depending on the O position relative to the Ni impurity. In general, for the Ni $3d^8$ configuration, the triplet ground state with $L_z = 0$ is the most stable in the *ab initio* calculations and is further stabilized by correlations. Therefore in this section, we analyze this case in more detail. The situation with two degenerate triplets with $L_z = \pm 1$ is very similar to the physics of an organic molecule in a metallic substrate and will be addressed in Sec. V.

To be specific, the system we are interested in, represented by the first row of Table I, namely "sym O–4th nn", is the one in which the symmetries of the Ni holes are well defined in the orbitals $\alpha = yz, xz$. Moreover, this case presents a larger hybridization with the host as can be seen in the broader density of states of these orbitals, see Fig. 3, leading to a larger Kondo scale. Taking into account the *ab initio* results presented in the previous section, the charge fluctuations in the Ni impurity are mainly due to the interchange between the state with two holes and virtual excitations to states with only one hole in either the $3d_{yz}$ or $3d_{xz}$ orbital (see Fig. 4). Furthermore, both configurations are magnetic with spin $S = 1$ and $S = 1/2$ for two and one holes, respectively. The spin-orbit coupling (SOC) in the Ni atom induces a splitting D between the projections $S_z = 1$ and $S_z = 0$ of the triplet that belongs to the total spin $S = 1$.

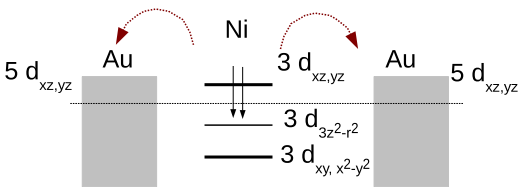

FIG. 4. (Color online) Schematic representation of Ni holes and their tunneling to the Au leads for the case "sym O–4th nn".

With this information, we propose a Hamiltonian that describes the system, and that is given by [39]

$$H = \sum_{M_2} \left(E_2 + DM_2^2\right)|M_2\rangle\langle M_2| + \sum_{\alpha M_1} E_\alpha |\alpha M_1\rangle\langle \alpha M_1| + \sum_{\nu k\alpha\sigma} \epsilon_{\nu k} c^\dagger_{\nu k\alpha\sigma} c_{\nu k\alpha\sigma} + \sum_{M_1 M_2} \sum_{\alpha\nu k\sigma} V_\nu \left\langle 1M_2 \left| \frac{1}{2}\frac{1}{2} M_1 \sigma \right.\right\rangle \times \left(|M_2\rangle\langle \alpha M_1| c_{\nu k\alpha\sigma} + \text{H.c.}\right), \quad (1)$$

where E_i and M_i represent the energies and the spin projections along the chain, chosen as the quantization axis, of states with $i = 1,2$ holes in the $3d$ shell of the Ni impurity. The state with two holes and maximum spin projection is denoted by $|1\rangle = \hat{d}^\dagger_{xz\downarrow}\hat{d}^\dagger_{yz\downarrow}|0\rangle$, where $|0\rangle$ represents the $3d^{10}$ configuration and the operator $\hat{d}^\dagger_{\alpha\sigma}$ creates a hole with symmetry $\alpha = xz, yz$ and spin projection σ. The states with one hole in the Ni atom can be constructed by removing an α hole. The other relevant states with two and one holes can be obtained by using the spin lowering operators.

The operator $c^\dagger_{\nu k\alpha\sigma}$ creates a hole in the $5d$ shell of the Au atom with symmetry α, where $\nu = L, R$ denotes the left or the right side of the Ni atom, respectively. The hopping V_ν characterizes the tunneling between the Ni and Au states.

Kondo regime

To describe the spin fluctuations, i.e., the Kondo regime in which the charge fluctuations are frozen, we perform a Schrieffer-Wolff transformation. The effective low energies' Hamiltonian is then

$$H_{\text{eff}} = \sum_{\nu\alpha\nu} \epsilon_{\nu k} c^\dagger_{\nu k\alpha\sigma} c_{\nu k\alpha\sigma} + \sum_{\alpha\nu} \frac{|V_\nu|^2}{2} \left\{ \frac{|1\rangle\langle 1| + |-1\rangle\langle -1|}{E_1 - D - E_2} + \frac{|0\rangle\langle 0|}{E_1 - E_2} \right\} \hat{n}_{c\alpha\nu} + J_\parallel \sum_\alpha S_z s^z_\alpha + J_\perp \sum_\alpha \left(S_x s^x_\alpha + S_y s^y_\alpha\right), \quad (2)$$

where $\hat{n}_{c\alpha\nu} = \sum_{k\sigma} c^\dagger_{\nu k\alpha\sigma} c_{\nu k\alpha\sigma}$, the spin of the xz orbital is $\mathbf{s}_{xz} = \sum_{\gamma\beta} d^\dagger_{xz\gamma} \boldsymbol{\sigma}_{\gamma\beta} d_{xz\beta}/2$ where γ and β are spin indices, and similarly for the yz orbital. $J_\parallel = \frac{|V|^2}{E_1 - E_2 - D}$, $J_\perp = 1/2(\frac{|V|^2}{E_1 - E_2 - D} + \frac{|V|^2}{E_1 - E_2})$, and $|V|^2 = (|V_L|^2 + |V_R|^2)/2$. The middle term represents a renormalization of the local energies and the potential scattering and is unimportant for understanding the Kondo effect. The final term represents the exchange interaction between the impurity spin S and the corresponding ones of the O-doped Au bands s_α, $J_\parallel$ and $J_\perp$ being the longitudinal and perpendicular couplings. This exchange term corresponds to the anisotropic Kondo Hamiltonian, H_K:

$$H_K = J_\parallel \sum_\alpha S_z s^z_\alpha + J_\perp \sum_\alpha \left(S_x s^x_\alpha + S_y s^y_\alpha\right). \quad (3)$$

Notice that in the absence of any anisotropy interaction, $D = 0$, the model reduces to $JS \cdot (s_{yz} + s_{xz})$, which is a

spin-1 two-channel, $n = 2$, Kondo model with $J = \frac{|V|^2}{E_1 - E_2}$, which is a Fermi liquid [21–24,40]. The Kondo temperature for our model can be estimated from the usual expression $T_K \sim e^{1/2J\rho_c(E_F)}$ in which $\rho_c(E_F)$ corresponds to the value of the density of states of the conduction band at the Fermi level, E_F. The only change with those associated to the spin-1/2 one-channel model enters in the change of the exchange coupling J, a half in our case as compared to the spin-1/2 one-channel [41].

For a numerical evaluation in terms of the *ab initio* parameters we use the fact that $J\rho_c(E_F) = \frac{\Delta}{\pi\epsilon_d}$, being $\Delta = \pi V^2 \rho_c(E_F)$ and $\epsilon_d = E_1 - E_2 \sim -E_{xz}$. We estimate Δ from the half maximum width of the $3d_\alpha$ density of states, which corresponds to $2\Delta \sim 0.23$ eV, and $|E_{xz}| \sim 0.23$ eV from its energy position. Thus, we estimate a Kondo temperature close to $T_K \sim 400$ K, and therefore the zero-bias anomaly should be observed in transport measurements.

As stated in Sec. II, we find that the value of the anisotropy constant D is of the order of $D \sim 15$ meV ~ 180 K. Studies of similar models by the numerical renormalization group suggest that for $D < T_K$ (as in this case) an energy scale D^* much smaller than D is dynamically generated. For example, for the underscreened $S = 1$ Kondo model with positive D, $D^* \approx \exp[-c(T_K/D)^{1/2}]$. While for $D = 0$ the conductance reaches its maximum value at $T = 0$, when $D \neq 0$ and for $T < D^*$ the conductance drops abruptly [27]. A similar D^* was found in an underscreened $S = 3/2$ model which displays non-Fermi-liquid behavior for $T < D^*$ [19].

Thus, while for temperatures above D^*, the model exhibits the features of the isotropic $S = 1$ two-channel model, and the splitting of the triplet states can be in practice neglected for $T \gg D^*$, at temperatures below D^* one expects a change of regime and a drop in the conductance. This is a general feature of the models for which the spin degeneracy of the impurity is removed [28], as in the underscreened $S = 1$ Kondo model with anisotropy [27].

V. SUMMARY AND DISCUSSION

By means of *ab initio* calculations we determined that in a Au chain an O doping of 14% is enough to push the Au $5d$ bands towards the Fermi level. With this amount of O atoms, the $5d_{xz,yz}$ orbitals of all the Au atoms present in the chain are conduction bands, normally below the Fermi level when not doped. Within this minimal concentration of dopants, we studied the effect of the O atoms on the spin state of a Ni magnetic impurity embedded in the O-doped Au chain, as well as the symmetry properties of the unoccupied bands (holes). We showed that when the O atoms are fourth neighbors of the Ni impurity, the $S = 1$ spin state of the Ni atom comes from its $3d_{xz,yz}$ empty states. This is a triplet with total angular momentum projection $L_z = 0$. Upon approaching the O atoms towards the Ni impurity, the $3d_{xz,yz}$ begin to be filled, while the $3d_{z^2}$ starts to be unoccupied, preserving the $S = 1$ spin. Therefore a transition to a Ni $3d^8$ configuration with two triplets with $L_z = \pm 1$ becomes possible, although correlations stabilize the $L_z = 0$ triplet.

After the description of the system and of the first-principles calculations, we introduced a mixed valence model for the Ni-O-Au chain in the substitutional configuration for Ni, assuming that the Ni impurity for two holes is in the $L_z = 0$ state. This can be viewed as a generalized Anderson impurity model, which includes not only the charge fluctuations (between $3d^8$ and $3d^9$ Ni configurations) but also the spin ones. By means of a Schrieffer-Wolff transformation we prove that the model can be mapped onto a two-channel spin-1 Kondo model. The SU(2) symmetry of the conduction channels of the O-doped Au chain allows for a full screening of the spin of the Ni impurity. We found that the associated Kondo temperature is experimentally accessible and that it is of the order of $T_K \sim 400$ K. Therefore, at low enough temperatures as compared with the Kondo one, the system behaves as a Fermi liquid and a zero-bias anomaly should appear in transport measurements. We also found that even if the low-energy model corresponds to an anisotropic one, the expected behavior should be similar to the isotropic case due to the fact that the anisotropy constant is found to be smaller than the isotropic Kondo temperature. A small energy scale D^* is dynamically generated, below which the conductivity should drop. We hope that this work stimulates an accurate many-body calculation of D^* which might be compared with the $D^* \approx \exp[-c(T_K/D)^{1/2}]$ behavior obtained in similar models [19,27].

As pointed out in the seminal work by Nozières and Blandin [40], if the relation $n = 2S$ is satisfied (as is actually the case), then, at temperatures below the characteristic one given by the Kondo temperature, $T \ll T_K$, the physics of the system is expected to be the same as that for a Fermi liquid. This is an example of a fully screened higher spin Kondo effect. Most of the transition metals in bulk conducting materials are described by this kind of totally screened Kondo phenomena [41]. However, this is not the usual behavior in low dimension and therefore our model represents a possible experimental realization of this kind of physics. Other low-dimensional examples of a two-channel spin-1 Kondo effect can be found in quantum dots (QDs). Specifically, Pustilnik and Glazman [42,43] studied the possibility of having a spin-1 QD coupled to two screening channels which fully screen the QD spin. However, they found that even with a small difference between the two antiferromagnetic coupling constants (which corresponds to a real situation), the physics of the QD is expected to be dominated by the underscreened one-channel spin-1 Kondo model, leading to a two-stage Kondo effect [44]. Fortunately, our model based on the O-doped Au chain has the advantage of having a protected SU(2) symmetry between the two conducting channels due to the cylindric symmetry.

The case with two degenerate triplets in the $3d^8$ configuration, in which one hole occupies the $3d$ orbital of z^2 symmetry and the other one can be occupied by another hole with xz or yz symmetry, is completely analogous to the case of iron(II) phtalocyanine molecules on Au(111) [29]. In this case, due to the different hybridization of the Fe orbitals with the substrate (as in our case, the hopping is larger for the z^2 orbital), a two-stage Kondo effect takes place. First, the spin of the z^2 orbital is screened. It is difficult for us to estimate the Kondo scale for this screening due to the uncertainty in the position of

the $3d_{z^2}$ state. The remaining degrees of freedom, the orbital (xz or yz) degeneracy, and spin 1/2 of the remaining hole are screened in a rather exotic SU(4) Kondo effect. The effects of the orbital degeneracy become evident when the molecules are assembled in a lattice [45–47]. It would be certainly interesting to find an SU(4) Kondo effect in nanoscopic chains.

ACKNOWLEDGMENTS

This work was partially supported by PIP No. 112-200801-01821, No. 00273, No. 112-201201-00069, and No. 00832 of CONICET, and PICT 2010-1060 and 2013-1045 of the ANPCyT, Argentina.

[1] A. I. Yanson, G. Rubio-Bollinger, H. E. van den Brom, N. Agraït, and J. M. van Ruitenbeek, Nature (London) **395**, 783 (1998).
[2] H. Ohnishi, Y. Kondo, and K. Takayanagi, Nature (London) **395**, 780 (1998).
[3] R. H. M. Smit, C. Untiedt, A. I. Yanson, and J. M. van Ruitenbeek, Phys. Rev. Lett. **87**, 266102 (2001).
[4] G. Rubio-Bollinger, S. R. Bahn, N. Agraït, K. W. Jacobsen, and S. Vieira, Phys. Rev. Lett. **87**, 026101 (2001).
[5] M. Ryu and T. Kizuka, Jpn. J. Appl. Phys. **45**, 8952 (2006).
[6] R. Vardimon, M. Klionsky, and O. Tal, Nano Lett. **15**, 3894 (2015).
[7] F. Barnett, H. Haekkinen, A. Scherbakov, and U. Landman, Nano Lett. **4**, 1845 (2004).
[8] F. D. Novaes, A. J. R. da Silva, E. Z. da Silva, and A. Fazzio, Phys. Rev. Lett. **96**, 016104 (2006).
[9] S. R. Bahn, N. Lopez, J. K. Nørskov, and K. W. Jacobsen, Phys. Rev. B **66**, 081405(R) (2002).
[10] W. H. A. Thijssen, D. Marjenburgh, R. H. Bremmer, and J. M. van Ruitenbeek, Phys. Rev. Lett. **96**, 026806 (2006).
[11] S. D. Napoli, A. Thiess, S. Blügel, and Y. Mokrousov, J. Phys.: Condens. Matter **24**, 135501 (2012).
[12] S. V. Aradhya, M. Frei, A. Halbritter, and L. Venkataraman, ACS Nano **7**, 3706 (2013).
[13] O. Cespedes, M. Wheeler, T. Moorsom, and M. Viret, Nano Lett. **15**, 45 (2015).
[14] P. Lucignano, R. Mazzarello, A. Smogunov, M. Fabrizio, and E. Tosatti, Nat. Mater. **8**, 563 (2009).
[15] Y. Miura, R. Mazzarello, A. Dal Corso, A. Smogunov, and E. Tosatti, Phys. Rev. B **78**, 205412 (2008).
[16] L. G. C. Rego, A. R. Rocha, V. Rodrigues, and D. Ugarte, Phys. Rev. B **67**, 045412 (2003).
[17] N. Agraäit, A. Yeyati, and J. van Ruitenbeek, Phys. Rep. **377**, 81 (2003).
[18] S. D. Napoli, M. Barral, P. Roura-Bas, A. Aligia, Y. Mokrousov, and A. Llois, IEEE Trans. Magn. **49**, 4683 (2013).
[19] S. Di Napoli, A. Weichselbaum, P. Roura-Bas, A. A. Aligia, Y. Mokrousov, and S. Blügel, Phys. Rev. Lett. **110**, 196402 (2013).
[20] S. Di Napoli, P. Roura-Bas, A. Weichselbaum, and A. A. Aligia, Phys. Rev. B **90**, 125149 (2014).
[21] P. Schlottmann and P. D. Sacramento, Adv. Phys. **42**, 641 (1993).
[22] N. Andrei and C. Destri, Phys. Rev. Lett. **52**, 364 (1984).
[23] A. M. Tsvelick and P. B. Wiegmann, J. Stat. Phys. **38**, 125 (1985).
[24] A. Jerez, N. Andrei, and G. Zaránd, Phys. Rev. B **58**, 3814 (1998).
[25] P. Mehta, N. Andrei, P. Coleman, Borda, and G. Zaránd, Phys. Rev. B **72**, 014430 (2005).
[26] E. Sela, A. K. Mitchell, and L. Fritz, Phys. Rev. Lett. **106**, 147202 (2011).
[27] P. S. Cornaglia, P. Roura-Bas, A. A. Aligia, and C. A. Balseiro, Europhys. Lett. **93**, 47005 (2011).
[28] R. Žitko, R. Peters, and T. Pruschke, Phys. Rev. B **78**, 224404 (2008).
[29] E. Minamitani, N. Tsukahara, D. Matsunaka, Y. Kim, N. Takagi, and M. Kawai, Phys. Rev. Lett. **109**, 086602 (2012).
[30] P. Blaha, K. Schwarz, G. K. H. Madsen, D. Kvasnicka, and J. Luitz, *Wien2k, an Augmented Plane Wave + Local Orbitals Program for Calculating Crystal Properties* (TU Wien, Wien, Austria, 2001).
[31] J. Perdew, S. Burke, and M. Ernzerhof, Phys. Rev. Lett. **77**, 3865 (1996).
[32] G. Sclauzero and A. Dal Corso, Phys. Rev. B **87**, 085108 (2013).
[33] M. A. Barral, P. Roura-Bas, A. M. Llois, and A. A. Aligia, Phys. Rev. B **82**, 125438 (2010).
[34] K. K. H. Eschrig, M. Sargolzaei, and M. Richter, Europhys. Lett. **72**, 611 (2005).
[35] O. Eriksson, M. S. S. Brooks, and B. Johansson, Phys. Rev. B **41**, 7311(R) (1990).
[36] G. Nicolas, J. Dorantes-Dávila, and G. M. Pastor, Phys. Rev. B **74**, 014415 (2006).
[37] A. A. Aligia, Phys. Rev. B **88**, 075128 (2013).
[38] A. A. Aligia and T. Kroll, Phys. Rev. B **81**, 195113 (2010).
[39] A. A. Aligia, C. A. Balseiro, and C. R. Proetto, Phys. Rev. B **33**, 6476 (1986).
[40] P. Nozières and A. Blandin, J. Phys. (France) **41**, 193 (1980).
[41] A. H. Nevidomskyy and P. Coleman, Phys. Rev. Lett. **103**, 147205 (2009).
[42] M. Pustilnik and L. I. Glazman, Phys. Rev. Lett. **87**, 216601 (2001).
[43] M. Pustilnik and L. I. Glazman, J. Phys.: Condens. Matter **16**, R513 (2004).
[44] A. Posazhennikova, B. Bayani, and P. Coleman, Phys. Rev. B **75**, 245329 (2007).
[45] N. Tsukahara, S. Shiraki, S. Itou, N. Ohta, N. Takagi, and M. Kawai, Phys. Rev. Lett. **106**, 187201 (2011).
[46] A. M. Lobos, M. Romero, and A. A. Aligia, Phys. Rev. B **89**, 121406 (2014).
[47] J. Fernández, A. A. Aligia, and A. M. Lobos, Europhys. Lett. **109**, 37011 (2015).